ENHANCED VISION OF HAZY IMAGES USING ADVANCED DEPTH ESTIMATION AND COLOR ANALYSIS

N.Krishna Prasad M.E, Assistant professor, ECE department, prasad42tech@gmail.com
1.R.Rashmi,ECE department,rashmirose650@gmail.com
2.G.Reshmai, ECE department, reshmagajendrarajan@gmail.com
3.T.Sirajunisha, ECE department, sirajunisha267@gmail.com

ABSTRACT

***Abstract*—Images captured during sandstorm conditions frequently feature degraded visibility and undesirable color cast effects. In such situations, traditional visibility restoration approaches usually cannot adequately restore images due to poor estimation of haze thicknessand the persistence of color cast problems. In this paper, we present a novel Laplacian-based visibility restoration approach to effectively solve inadequate haze thickness estimation and alleviate color cast problems. By doing so ,a high-quality image with clear visibility and vivid colorcan be generated. Experimental results via qualitative and quantitative evaluations demonstrate that the proposed method can dramatically improve images captured during inclement weather conditions and produce results superior to those of other state-of-the-art methods.**

***Index Terms*—Gamma correction, Laplacian distribution,**
Retinex theory, visibility restoration

I.INTRODUCTION

DURING inclement weather conditions such as fog, sand,and mist, captured images will exhibit degraded visibility.

This is because the suspended particles absorb and scatter specific spectrums of light between the observed objects and the digital camera. Accordingly, these degraded images can directly reduce the performance quality of systems such as object recognition systems [1]–[3], obstacle detection systems

[4]–[6], video surveillance systems [7]–[12], intelligent transportation systems [13]–[15], and so on [16]. Numerous visibility restoration approaches have been proposed to restore the visibility of degraded images in order to improve system performance during inclement weather conditions [17]. These visibility restoration approaches can further be divided into additional information approaches [18]–[20], multiple-image approaches [21]–[23], and single-image approaches [24]–[29].

Additional information approaches restore hazy images by using given scene depth information obtained from either an additional operation or user interaction, such as through user operation

to control camera positions and via a given approximate 3-D geometrical model. However, these approaches are notwell-suited for real-world application due to limitations placed

on the acquisition of scene depth information by unknown geography information and additional user operation. Multipleimageapproaches adopt two or more images of the same scene, which are captured by using specific hardware, e.g., a rotating polarizing filter, to effectively construct the scene depth information and further achieve visibility restoration of incoming hazy images. Unfortunately, the use of thesemultiple image approaches usually requires either excessive hardware expense or special devices.

Recently, many studies have focused on single-image approaches to restore the visibility of a hazy image. These approaches are based on either strong assumptions or robust priors, by which haze thickness is estimated by using only a single image. Tan [24] observed that a haze-free image possesses evident contrasts compared with a hazy image. By using observations of scene contrast changes, the method of

Tan restores the visibility of an image by maximizing its local contrast. However, the images restored by this method often feature serious artifacts along depth edges.

Another work proposed by Fatal [25] restores the visibility of hazy images by estimating the albedo of a scene and inferring the transmission medium. This was accomplished via the assumption that the transmission medium and the surface shading are locally uncorrelated. Nevertheless, the method of Fatal usually fails at restoration when the incoming images contain heavy haze formation. He *et al.* [26] observed that, with the exception of sky regions, an outdoor haze-free image features at least one spectrum in the RGBcolor channels that exhibits a very low intensity value within patches of the image. Inspired by this observation, they propose the dark channel prior (DCP)method by which to effectively estimate the thickness of hazeinformation and further

restore scene radiance. Until now, the method of He *et al.* has received the most attention due to its relative success in restoring visibility in hazy images
.

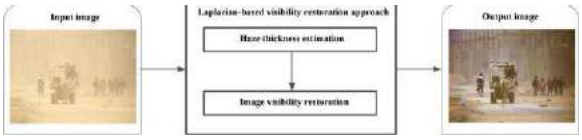

Fig. 1.Flowchart of the proposed Laplacian-based visibility restoration approach.haze-free images withoutgeneration of any block effects forhazy image captured in foggy weather conditions. However,they usually fail in restoring the visibility of images whose hazeis the result of capture during sandstorm conditions. This is dueto the hindrance of restoration ability by color cast problemsand insufficient estimation of haze thickness.

This paper proposes a novel DCP-based visibility restoration technique that exploits the advantages of the proposed hazethickness estimation (HTE) module and the proposed image visibility restoration (IVR) module and combines them in order to effectively overcome color cast problems and insufficient estimation of haze thickness. In contrast with traditional DCP based techniques, the proposed technique is built on a Laplacianstrategy. Based on this strategy, the proposed method is able to more effectively produce a haze-free image than can the traditional DCP-based techniques. The following are the key features of our proposed method.

1) First, the proposed HTE module is used to avoid insufficient estimation of haze thickness in real-world sandstorm conditions. This module is based on the
Laplacian-based gamma correction technique and can effectively estimate the thickness of haze formation, which subsequently refines the transmission map.

2) After haze thickness is effectively calculated in the proposed
HTE module, the proposed IVR module is applied via Laplacian-based white patch-Retinex technique to effectively recover true scene colors. Hence, a haze-free image can be effectively generated by the proposed method.

As demonstrated by both qualitative and quantitative analysis of the experimental results, the efficacy of visibility restoration via the proposed method for images captured under various climatic conditions is superior to those of the other DCP-based techniques proposed in [26]–[29].

The rest of this paper is structured as follows. A brief description of the optical model is presented for computer vision in Section II. Moreover, Section III describes in detail the proposed method for visibility restoration in a wide range of weather conditions. Section IV presents the experimental results of qualitative and quantitative analysis of the proposed method and the other state-of-the-art DCP-based methods.

Finally, we give our concluding remarks in Section V.

II. Background

A. Optical Model

The intention of this section is to introduce an optical model that describes the formation of hazy images and is widely used
in the field of computer vision. The model can be expressed as follows:

$I(x) = J(x)t(x) + A(1 - t(x))$ (1) where $I(x)$ represents the hazy image captured by the digital camera; $J(x)$ represents the scene radiance, which can be regarded as a haze-free image; A represents the global atmospheric light; x represents each pixel location of the incoming image; and $t(x)$ represents transmission map, which is used to describe the nonscattered light between the observed objects and the digital camera.

Note that the first term $J(x)t(x)$ and the second term $A(1 - t(x))$ of (1) represent the direct attenuation and the airlight, respectively [26]. The decay of scene radiance
$J(x)$ can be described by direct attenuation, which is subject to medium and scene depth information.

Moreover, the airlight value usually suffers from scattering and absorption by atmospheric particles, resulting in scene
color variation. When the atmosphere considered here is assumed to be homogenous, the transmission map $t(x)$ can be expressed as $t(x) = e^{-\beta d(x)}$ (2)

III. Proposed Method

Here, we propose a novel visibility restoration approach based on the Laplacian strategy in order to restore hazy images captured in real-world inclement weather conditions. To this end, the proposed approach consists of two major modules, i.e., an HTE module and an IVR module.

As illustrated in Fig. 1, the proposed HTE module is first employed via a combination of the Laplacian distribution model and gamma correction technique to refine the transmission map for overcoming the insufficient estimation of haze thickness.

Next, the proposed IVR module is utilized, which is basedon a combination of the Laplacian distribution model andwhite patch-Retinex theory to estimate the adjustable colorparameters of the hazy image and

further overcome color cast problems in the restoration result. Finally, a haze-free image can be generated by using the refined transmission map and the estimated adjustable colorparameters to adequately remove atmospheric particles from hazy images.

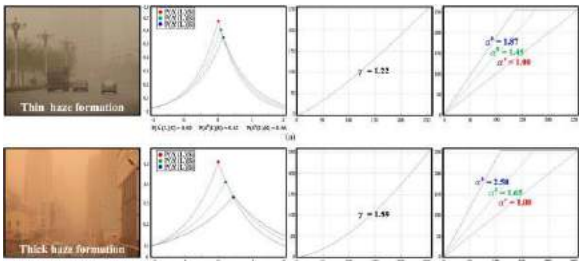

Fig. 2.Characteristics of the Laplacian distribution model, the proposed self-adaptive parameters, and the proposed color adjustable parameters.

A. Haze Thickness Estimation

As was mentioned in the previous section, estimation of hazethickness during sandstorm conditions is a challenging task for traditional DCP-based methods, resulting in an insufficient transmission map.

To overcome this, the Laplacian-based gamma correction technique is proposed to flexibly refine the insufficient transmission map. To this end, we initially adopt the color cast detection technique [30] to examine whether color cast problems exist in the incoming hazy image. Subsequently, when an incoming image exhibits color cast problem, the Laplaciandistribution value $P(\Delta_c(L)/S)$ of each RGB color channel is calculated as follows:

$$P(\Delta(L)/S) = \frac{1}{a} \sum_{L \in S} \frac{1}{2\sigma} \exp\left(-|I_c(L) - \mu|/\sigma\right) \quad (3)$$

$$\Delta_c(L) = |I_M(L) - I_c(L)| \quad (4)$$

where $c \in \{r, g, b\}$, M represents the maximum value of each color channel within region S, $\Delta_c(L)$ represents the colorvariance, L represents a corresponding pixel within region S, and a represents the number of pixels in region S. Note that region S consists of the highest intensity values of the incoming image, which are selected from the top 0.1% brightest pixels in its dark channel. Here, μ and σ are the location and scale parameters of Laplacian distribution, respectively. When an image without color cast problems contains a consistent distribution for each RGB color channel, μ usually tends toward the slightest difference between each color channel. Additionally, the scale parameter σ can be defined for each pixel within region S as follows:

$$\sigma = \frac{1}{a} \sum_{L \in S} |I_c(L) - \mu| \quad . \quad (5)$$

According to the philosophy of Laplacian strategy in (3), an image with a slight colorcast possesses a high Laplaciandistribution value due to a smaller color variance of the image content, whereas an image with a heavy color cast possesses a low Laplacian distribution value due to the large color variance of its content, as shown in Fig. 2. Using this characteristic, we employ a gamma correction technique [31], [32] with selfadaptiveparameters to refine the insufficient transmission map $\tilde{t}(x)$, which is generated by using the DCP technique [26]. The refined transmission map $t(x)$ can be produced as follows:

$$t(x) = \left(\frac{\tilde{t}(x)}{I_{\max}}\right)^{r} \quad (6)$$

where $I_{\max}$ represents the maximum value of a pixel and can be set to 1, and $\tilde{t}(x)$ denotes an insufficient transmission map, which is acquired after using the soft-matting technique according to [26]. Note that γ represents the self-adaptive parameter and can be acquired based on the Laplacian distribution value as follows:

$$\gamma = \frac{P(\Delta_M(L)/S)}{P(\Delta_m(L)/S)} \quad (7)$$

where m and M represent the minimum value and the maximum value between the RGB color channels within region S,respectively. Moreover, a self-adaptive parameter γ that featureshigher values indicates superior refinement efficacy in the

insufficient transmission map $\tilde{t}(x)$, as illustrated in Fig. 2.

Note that there are more explanations about the role of the self adaptiveparameter γ in the next section.

B. Image Visibility Restoration

After the Laplacian distribution values and refined transmission map are generated in the proposed HTE module, the proposed IVR module can effectively recover visibility in the restored image. In general, the image captured in sandstorm conditions usually contains color cast problems featuring insufficient amounts of color variation. However, traditional DCP based methods proposed in [26]–[29] are unable to overcome these color cast problems, which results in these problems in their restored images, as discussed in the previous section.

To avoid color cast problems in restored images, we employ the Laplacian-based white patch-Retinex technique to effectively recover true scene color in sandstorm images because the white patch-Retinex theory is well-suited for images with insufficient amounts of color variations according to [33]. To this end, we combine information of both the Laplacian distribution values and the white patch-Retinex theory to estimate the adjustable color parameters α_c as follows: $\alpha_c =$

$V_c$max

$_cI_c$(where

$v_c=\Delta_M(L)/SP$ $(\Delta_c(L)/S)$(9and $c \in \{r, g, b\}$. Note that max$_cI_c$represents the maximum intensity of each RGB color channel in the hazy image; $v_c$are the chromatic adaptable parameters; m and M represent the minimum and maximum values between the RGB colorchannel within region S, respectively. Moreover, the chromatic adaptable parameter with higher values indicates inconsistent distributions of the color channel in the incoming image, as indicated in Fig. 2. Finally, a high-quality image can be generated during the proposed IVR module via the conjunctive utilization of the

color adjustable parameters α_c and the refined transmission map t produced by the proposed HTE module. Thus, the restoration function can be formulated by

$J_c(x) = \alpha_c (I_c(x) - A_c)$ max $(t(x), t_0)$

Based on our first observation, there is a positive correlation between serious color cast problems and insufficient estimation of haze thickness in the transmission map. Therefore, the transmission map of Fig. 2(b) usually requires superior compensation efficacy for the intensity value when compared with the transmission map of Fig. 2(a). As shown in Fig. 2(b), due to the fact that the image contains serious color cast effects, the self-adaptive parameters γ often tend toward a higher value compared with Fig. 2(a) according to (6) and (7). Accordingly, the transmission map of Fig. 2(b) requires more compensation,as self-adaptive parameters possess larger variation values.

According to our second observation, the RGB color channels become more inconsistent as color cast problems increase in severity in images captured during sandstorm conditions. Accordingly, as shown in Fig. 2(b), the adjustable color parameter α possesses a higher value for green and blue color channels since the incoming image features serious color cast problem and inconsistent distribution between the RGB color channel, as compared with Fig. 2(a), according to (8) and (9). Compared with Fig. 2(a), the distribution for green and blue color channels can be substantially adjusted, as shown in Fig. 2(b).

Based on these characteristics, the proposed HTE module and the proposed IVR module are able to flexibly refine the insufficient transmission map and recover true scene color,

+ α_cA_c(10) where $c \in \{r, g, b\}$, $J_c(x)$ represents the scene radiance, $I_c(x)$represents the hazy image captured by the digital camera, $A_c$represents the global atmospheric light, α_c represents the coloradjustable parameters, and t_0 represents the lower bound of the refined transmission map t. Here, t_0 can be set to 0.1. For more details of t_0, please refer to the literature [26].

Fig. 2 presents the analysis of the Laplacian distribution model, the proposed self-adaptive parameters γ, and the proposed

color adjustable parameters α for two hazy images captured during sandstorm conditions, and which consequently feature color cast problems. As can be observed in Fig. 2(a) and

(b), it is obvious that the color cast problem in Fig. 2(b) is more serious than the color cast problem in Fig. 2(a). In addition, when the self-adaptive parameters and color adjustable parameters based on the Laplacian distribution model possess lower variation values, the corresponding incoming hazy image will feature only a slight color cast. In contrast, the self-adaptive parameters and the color adjustable parameters based on the

Laplacian distribution model that possesses larger variation

A. Qualitative Evaluation

As shown in Figs. 3–8, images restored via each of the
DCP-based methods proposed in [26]–[29] and the proposed method were measured through visual evaluation of six sandstorm images titled "Carriage," "Downtown," "Pedestrian,"
Street," "City," and "Park." During sandstorm conditions, captured images usually exhibit significant color cast effects and inconsistent distributions of the RGB color channels due

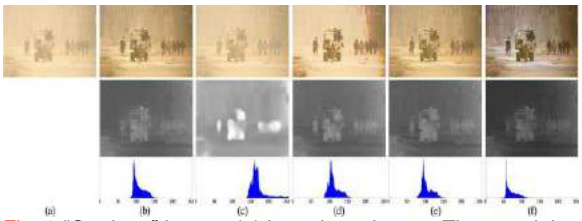

Fig. 3."Carriage" image. (a) Input haze image. The remaining five images are the restoration results with corresponding transmission maps and
their respective statistical histograms generated by the methods of (b) He *et al.* [26], (c) Xie*et al.* [27], (d) Xu*et al.* [28], (e) Jin *et al.* [29], and
(f) the proposed method.

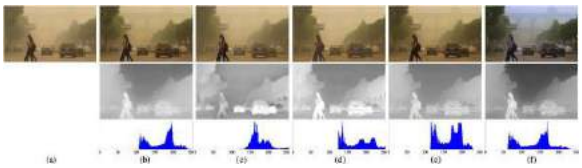

Fig. 4."Downtown" image. (a) Input haze image. The remaining five images are the restoration results with corresponding transmission maps and
their respective statistical histograms generated by the methods of (b) He *et al.* [26], (c) Xie*et al.* [27], (d) Xu*et al.* [28], (e) Jin *et al.* [29], and
(f) the proposed method

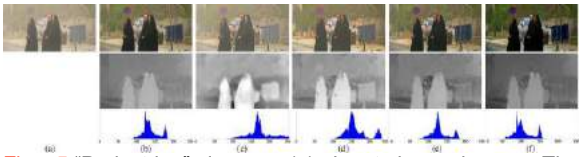

Fig. 5."Pedestrian" image. (a) Input haze image. The remaining five images are the restoration results with corresponding transmission maps
and their respective statistical histograms generated by the methods of (b) He *et al.* [26], (c) Xie*et al.* [27], (d) Xu*et al.* [28], (e) Jin *et al.* [29], and
(f) the proposed method

As shown in the first row of Figs. 3(b)–(e)–5(b)–(e), thebackground region of the hazy image containing the building, bridge, and tree, was still covered by atmospheric particles of sand after performance of the methods of He *et al.*, Xie*et al.*,
Xu*et al.*, and Jin *et al.* This is because the haze thickness is insufficiently estimated in the transmission map, which is shownin the second row of Figs. 3(b)–(e)–5(b)–(e). In contrast to the
DCP-based method, the proposed method can completely remove the sand particles and effectively recover the visibility of a degraded image, as displayed in the first row of Figs. 3(f)–5(f).
This is due to the proposed HTE module and its use of a
Lapacian-based gamma correction technique to effectively refine an insufficient transmission map, which can be observed in the second row of Figs. 3(f)–5(f). In addition, the statistical histograms of the transmission map for each compared method are shown in the third row of Figs. 3(b)–(e)–5(b)–(e).
The higher values in the transmission map represent thinner haze formation, whereas lower values represent thicker haze formation. It is obvious from the histograms that the proposed method produces lower intensity values in its transmission map than do the DCP-based methods, which means the estimation of haze thickness is more accurate, as shown in the third row of

B. Quantitative Evaluation

Quantifying the restored images is a very difficult task. This is because a real-world haze-free reference image has not been validated for quantification of restored images.
In general, the objective metrics used for quantitatively estimating the efficacy of the restoration results can be divided into two categories, i.e., reference methods and non-reference

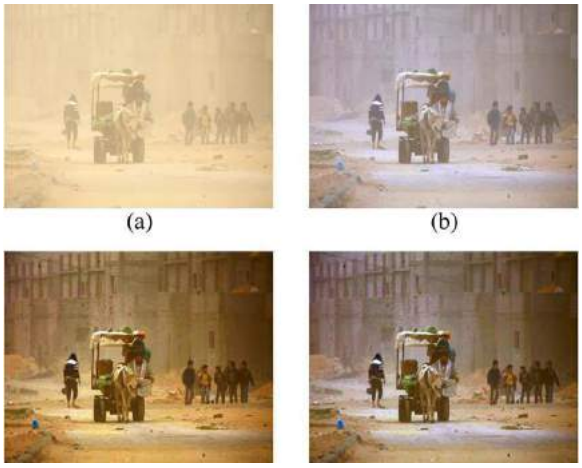

Fig. 9."Carriage" image restored by using the proposed HTE moduleand the proposed IVR module alone, respectively. (a) Input haze image.
(b) Restoration result produced by using only the proposed IVR module.
(c) Restoration result produced by using only the proposed HTE module.
(d) Restoration result produced by the proposed method via the use of both the proposed HTE module and the proposed IVR module.

However, as previously stated, a real-world hazefreereference image is unavailable for comparison of the restoration results between the proposed method and the DCP based methods proposed in [26]–[29]. Consequently, this paper adopted a non-reference method and mean opinion score to analyse restoration efficacy. First, three well-known quantitative metrics, i.e., e, $.r$, and σ, of the non-reference method are used to quantify the restored images. The e metric represents the rate of visible edge restoration in the haze-free image and is given by

$$e = \frac{V_r - V_o}{V_o} \quad (11)$$

where V_r and V_o represent the total number of visible edges within the restored hazy image and the incoming hazy image, respectively. Subsequently, $.r$ metric is used to express the quality of contrast restoration within the haze-free image. As such, the $.r$ metric is formulated as follows:

$$.r = \exp\left[\frac{1}{V_r} \sum_{P_i \in \wp r} \log(r_i)\right] \quad (12)$$

where P_i is the corresponding element within the set $\wp r$, and r_i is the rate of gradients between the restored hazy image and the incoming hazy image. Note that $\wp r$ consists of the visible edges in the restored hazy image. Moreover, the σ metric represents the number of pixels that might be either overexposed as white or underexposed as black in the restored image. The σ metric is calculated as follows:

$$\sigma = \frac{V_s}{\dim_x \dim_y} \quad (13)$$

where V_s represents the total of both overexposed and underexposed pixels in the restored image, and $\dim_x \dim_y$ represents the size of the incoming image.

In general, the use of these metrics can provide an objective comparison based on the total number of visible edges within the restored hazy image when the images restored

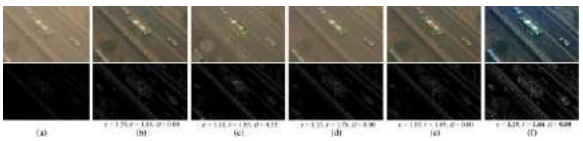

Fig. 10. "Highway" image. (a) Input haze image with its corresponding visible edges. The remaining five images are the restoration results with corresponding visible edges generated by the methods of (b) He *et al.* [26], (c) Xie*et al.* [27], (d) Xu*et al.* [28], (e) Jin *et al.* [29], and (f) the proposed method.

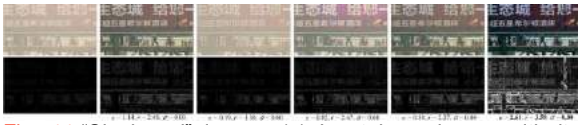

Fig. 11. "Signboard" image. (a) Input haze image with its corresponding visible edges. The remaining five images are the restoration results with corresponding visible edges generated by the methods of (b) He *et al.* [26], (c) Xie*et al.* [27], (d) Xu*et al.* [28], (e) Jin *et al.* [29], and (f) the proposed method.

V. Conclusion

In this paper, we have presented a novel Laplacian-based visibility restoration approach for restoration of degraded images captured during inclement weather conditions, such as fog and sandstorms. The proposed method is based on the Laplacian distribution model and features a combination of the proposed HTE module along with the proposed IVR module to adequately remove haze formation and recover vivid scene color in an image. Laplacian-based gamma correction is used during the proposed HTE module to refine an insufficient transmission map and thus achieve effective estimation of haze thickness, after which the refined transmission map is used to restore the visibility of a degraded image via the proposed IVR module. The proposed IVR module utilizes Laplacian based white patch-Retinex theory to equalize each RGB colorchannel and subsequently overcome color cast problems in restored images. Consequently, the proposed IVR module can effectively produce haze-free and vivid restoration results for degraded images captured during varied weather conditions.

Experimental results via qualitative and quantitative evaluations demonstrate that the proposed Laplacian-based visibility restoration approach is significantly superior to those of other of state-of-the-art methods. To the best of our knowledge, no such method exists for restoration of images captured in natural environments with varied weather conditions.

References

[1] R. C. Luo and C. L. Chun, "Multisensor fusion-based concurrent environment mapping and moving object detection for intelligent service robotics," *IEEE Trans. Ind. Electron.*, vol. 61, no. 8, pp. 4043–4051, Aug. 2014.

[2] H. Zhuang, K. S. Low, andW.Y.Yau, "Multichannel pulse-coupledneuralnetwork-based color image segmentation for object detection," *IEEE Trans. IndElectron.*, vol. 59, no. 8, pp. 3299–3308, Aug. 2012.

[3] H. H. Kim, D. J. Kim, and K. H. Park, "Robust elevator button recognition in the presence of partial occlusion and clutter by specular reflections,"
IEEE Trans. Ind. Electron., vol. 59, no. 3, pp. 1597–1611, Mar. 2012.
[4] H. Rezaee and F. Abdollahi, "A decentralized cooperative control scheme with obstacle avoidance for a team of mobile robots," *IEEE Trans. Ind.Electron.*, vol. 61, no. 1, pp. 347–354, Jan. 2014.
[5] J. S. Hu, J. J. Wang, and D. M. Ho, "Design of sensing system and anticipativebehavior for human following of mobile robots," *IEEE Trans.Ind. Electron.*, vol. 61, no. 4, pp. 1916–1927, Apr. 2014.
[6] S. Hong, Y. Oh, D. Kim, and B. J. You, "Real-time walking pattern generation method for humanoid robots by combining feedback and feed forward controller," *IEEE Trans. Ind. Electron.*, vol. 61, no. 1, pp. 355–364,
Jan. 2014.
[7] S. C. Huang, "An advanced motion detection algorithm with video quality analysis for video surveillance systems," *IEEE Trans. Circuits Syst. Video*
Technol., vol. 21, no. 1, pp. 1–14, Jan. 2011.
[8] X. Zhang, W. Hu, S. Chen, and S. Maybank, "Graph-embedding-based learning for robust object tracking," *IEEE Trans. Ind. Electron.*, vol. 61, no. 2, pp. 1072–1084, Feb. 2014.
[9] S. C. Huang and B. H. Chen, "Highly accurate moving object detection in variable-bit-rate video-based traffic monitoring systems," *IEEE Trans.Neural Netw. Learn. Syst.*, vol. 24, no. 12, pp. 1920–1931, Dec. 2013.
[10] M. Chacon and S. Gonzalez, "An adaptive neural-fuzzy approach for object detection in dynamic backgrounds for surveillance systems," *IEEE*
Trans. Ind. Electron., vol. 59, no. 8, pp. 3286–3298, Aug. 2012.
[11] S. C.Huang and B. H. Do, "Radial basis function based neural network
for motion detection in dynamic scenes," *IEEE Trans. Cybern.*, vol. 44, no. 1, pp. 114–125, Jan. 2014.
[12] S. C. Huang and B. H. Chen, "Automatic moving object extraction through a real-world variable-bandwidth network for traffic monitoring
systems," *IEEE Trans. Ind. Electron.*, vol. 61, no. 4, pp. 2099–2112,
Apr. 2014.
[13] S. C. Huang, B. H. Chen, and Y. J. Cheng, "An efficient visibility enhancement
algorithm for road scenes captured by intelligent transportation
systems," *IEEE Trans. Intell. Transp. Syst.*, vol. 15, no. 5, pp. 2321–2332,
Oct. 2014.
[14] J.-P. Tarel*et al.*, "Vision enhancement in homogeneous and heterogeneous
fog," *IEEE Trans. Intell. Transp. Syst. Mag.*, vol. 4, no. 2, pp. 6–20, 2012.
[15] Y. Kang, C. Roh, S. B. Suh, and B. Song, "A lidar-based decision-making method for road boundary detection using multiple Kalman filters," *IEEE*
Trans. Ind. Electron., vol. 59, no. 11, pp. 4360–4368, Nov. 2012.
[16] S. C. Huang, M. K. Jiau, and C. A. Hsu, "A high-efficiency and high-accuracy fully automatic collaborative face annotation system for distributed online social networks," *IEEE Trans. Circuits Syst. Video*
Technol., vol. 24, no. 10, pp. 1810–1813, Oct. 2014.
[17] S. C. Huang, B. H. Chen, andW. J.Wang, "Visibility restoration of single
hazy images captured in real-world weather conditions," *IEEE Trans.*
Circuits Syst. Video Technol., vol. 24, no. 10, pp. 1814–1824, Oct. 2014.
[18] K. Tan and J. P. Oakley, "Enhancement of color images in poor visibility conditions," in *Proc. IEEE ICIP*, Sep. 2000, vol. 2, pp. 788–791.
[19] S. G. Narasimhan and S. K. Nayar, "Interactive (De) weathering of an image using physical models," in *Proc. ICCV Workshop ColorPhotometr.Methods Comput. Vis.*, Oct. 2003, pp. 1387–1394.
[20] J. Kopf *et al.*, "Deep photo: Model-based photograph enhancement and
viewing," *ACM Trans. Graphics*, vol. 27, no. 5, pp. 116:1–116:10, Dec. 2008.
[21] Y. Y. Schechner, S. G. Narasimhan, and S. K. Nayar, "Polarization based vision through haze," *Appl. Opt.*, vol. 42, no. 3, pp. 511–525, Jan. 2003.
[22] S. G. Narasimhan and S. K. Nayar, "Contrast restoration of weather degraded images," *IEEE Trans. Pattern Anal. Mach. Intell.*, vol. 25, no. 6,
pp. 713–724, Jun. 2003.
[23] S. K. Nayar and S. G. Narasimhan, "Vision in bad weather," in *Proc. 7th*
IEEE ICCV, Jun. 1999, vol. 2, pp. 820–827.
[24] R. Tan, "Visibility in bad weather from a single image," in *Proc. IEEE*
Conf. CVPR, Jun. 2008, pp. 1–8.
[25] R. Fattal, "Single image dehazing," in *Proc. ACM SIGGRAPH*, 2008,
pp. 1–7.
[26] K. He, J. Sun, and X. Tang, "Single image haze removal using dark
channel prior," *IEEE Trans. Pattern Anal. Mach. Intell.*, vol. 33, no. 12,
pp. 2341–2353, Dec. 2011.
[27] B. Xie, F. Guo, and Z. Cai, "Improved single image dehazing using dark channel prior and multi-scale Retinex," in *Proc. Int. Conf. Intell. Syst.Des. Eng. Appl.*, Oct. 2010, pp. 848–851.
[28] H. Xu, J. Guo, Q. Liu, and L. Ye, "Fast image dehazing using improved dark channel prior," in *Proc. IEEE Int. Conf. Inf. Sci. Technol.*,Mar. 2012,
pp. 663–667.
[29] W. Jin, Z. Mi, X. Wu, Y. Hung, and X. Ding, "Single image de-haze based on a new dark channel estimation method," in *Proc. IEEE Int. Conf.*
Comput. Sci. Autom. Eng., May 2012, vol. 2, pp. 791–795.
[30] F. Gasparini and R. Schettini, "Color correction for digital photographs,"in *Proc. IEEE Int. Conf. Image Anal.Process.*, Sep. 2003, pp. 645–651.
[31] S. C. Huang, F. C. Cheng, and Y. S. Chiu, "Efficient contrast enhancement using adaptive gamma correction with weighting distribution," *IEEE*
Trans. Image Process., vol. 22, no. 3, pp. 1032–1041, Mar. 2013.
[32] S. C. Huang and W. C. Chen, "A new hardware-efficient algorithm and reconfigurable architecture for image contrast," *IEEE Trans. ImageProcess.*, vol. 23, no. 10, pp. 4426–4437, Oct. 2014.
[33] N. Banic and S. Loncaric, "Light random sprays Retinex: Exploiting the noisy illumination estimation," *IEEE Signal Process. Lett.*, vol. 20, no. 12,
pp. 1240–1243, Dec. 2013.
[34] Explore—Flickr. [Online]. Available: http://www.flickr.com/[35] Picasa Web Albums. [Online]. Available: http://picasa.google.com/
[36] Google Images. [Online]. Available: http://images.google.com/[37] N. Hautière, J.-P. Tarel, D. Aubert, and E. Dumont, "Blind contrast enhancement assessment by gradient rationing at visible edges," *ImageAnal.Stereol.*, vol. 27, no. 2, pp. 87–95, 2008.
[38] F. C. Cheng and S. C. Huang, "Efficient histogram modification usingbilateral Bezier curve for the contrast enhancement," *J. Display Technol.*,
vol. 9, no. 1, pp. 44–50, Jan. 2013.